

# Development of External RF Antenna based Cusp Free High Duty Factor Pulsed Negative Hydrogen Ion Source

Dharmraj V. Ghodke<sup>a,1</sup>, R. K. Khare<sup>1</sup>, Rajnish Kumar<sup>1,2</sup>, Manish Pathak<sup>1</sup>,  
S. K. Jain<sup>1,2</sup>, Ajith Amban<sup>1</sup>, K. Murali Krishnan<sup>1</sup>, Kuldeep Kumar Singh<sup>1</sup>,  
Purushottam Shrivastava<sup>1</sup> and Vijendra Prasad<sup>1</sup>

<sup>1</sup> *Proton Linac Development Division, Proton Accelerator Group,  
Raja Ramanna Centre for Advanced Technology,  
Indore - 452 013, India*

<sup>2</sup> *Homi Bhabha National Institute, Training School Complex, Anushakti Nagar,  
Mumbai - 400 094, India*

<sup>a</sup>Corresponding author: [dvghodke@rrcat.gov.in](mailto:dvghodke@rrcat.gov.in)

**Abstract.** An external RF antenna based cusp free negative hydrogen ( $H^-$ ) ion source has been designed and developed. This source is operated at 10% duty factor and the key experimental results are reported in the paper. The extracted  $H^-$  ion beam current is 11 mA with 2 ms pulse duration and 50 Hz repetition rate at 50 keV beam energy. Operation of the  $H^-$  ion source at high duty factor results in temperature rise in components, which may lead to failure of electronic components and vacuum joints of plasma chamber, igniter chamber and burn out of extraction electrodes. In order to keep the operating temperature within limits, water cooling system was designed and incorporated for (i) the 2 MHz RF antenna operating at 90 A RMS at 7 kV AC, (ii) the extraction electrodes, which is operating at maximum voltage of 15 kV DC, (iii) the plasma chamber (made of Aluminium Nitride, transparent to RF field with high thermal conductivity), and (iv) the Faraday cup for  $H^-$  ion current measurement. Forced air cooling was used for RF based pulsed igniter, operating at 13.56 MHz and various current stabilizing electrode biasing networks and RF impedance matching networks.

## INTRODUCTION

In negative hydrogen ( $H^-$ ) ion source, plasma is created mainly either by DC/pulsed arcing or electrodeless inductively coupled plasma method<sup>1-6</sup>. The  $H^-$  current is normally enhanced by creating thin layer of cesium on plasma electrode surface<sup>1</sup>. A minimum three electrodes system (triode), namely plasma, extraction and ground electrodes are required for  $H^-$  ion beam extraction<sup>7</sup>. Einzel lens and chopper are normally introduced in electrode geometry to shape the extracted  $H^-$  ion current<sup>1,2,7-9</sup>. Permanent Magnet (PM) or electromagnets are used in plasma generating system for confinement and to enhance the plasma density along the beam extraction axis<sup>9-12</sup>. A filter field is introduced in plasma chamber to reduce the high energy electrons reaching towards the plasma electrode. The co-extracted electrons are terminated on extraction electrode using dipole magnetic field using PM. An igniter is generally required for reliable pulsed mode operation of main plasma<sup>4</sup>. The igniter generates weak plasma either by DC current glow discharge or by 13.56 MHz RF discharges. This weak plasma electrons and ions act as seed for main plasma. The main plasma density increased by high current DC or RF power, in order to increase the extracted  $H^-$  ion current.

This paper describes the external RF antenna based cusp free high duty factor pulsed  $H^-$  ion source. To operate ion source at high duty factor, efficient cooling arrangement is required. Hence, water-cooling arrangement is provided for extraction electrode, 2 MHz RF antenna, plasma electrode and main plasma chamber. Forced air cooling is provided for igniter, RF matching networks and high voltage current stabilizing networks. The developed  $H^-$  ion source was tested in two modes, i.e. low duty factor (0.4%) operation to extract 15 mA ion current at 2 Hz repetition rate and high duty factor (10%) operation to extract 11 mA ion current at 50 Hz repetition rate, both with 2 ms pulse width and at 50 keV energy as given in table 1. The  $H^-$  ion source was developed to operate in pulsed mode for Indian facility for spallation research.

**TABLE 1.** The measured parameters of external RF antenna based  $H^-$  ion source.

Description	Low Duty Cycle Operation	High Duty Cycle Operation
Particles	$H^-$	$H^-$
Beam Energy	50 keV	50 keV
Beam Current	15 mA	11 mA
Main Plasma Chamber Frequency	2 MHz	2 MHz
Igniter Frequency	13.56 MHz	13.56 MHz
Pulse Width	2 ms	2 ms
Pulse Repetition Rate	2 Hz	50 Hz
Duty Factor	0.4%	10%

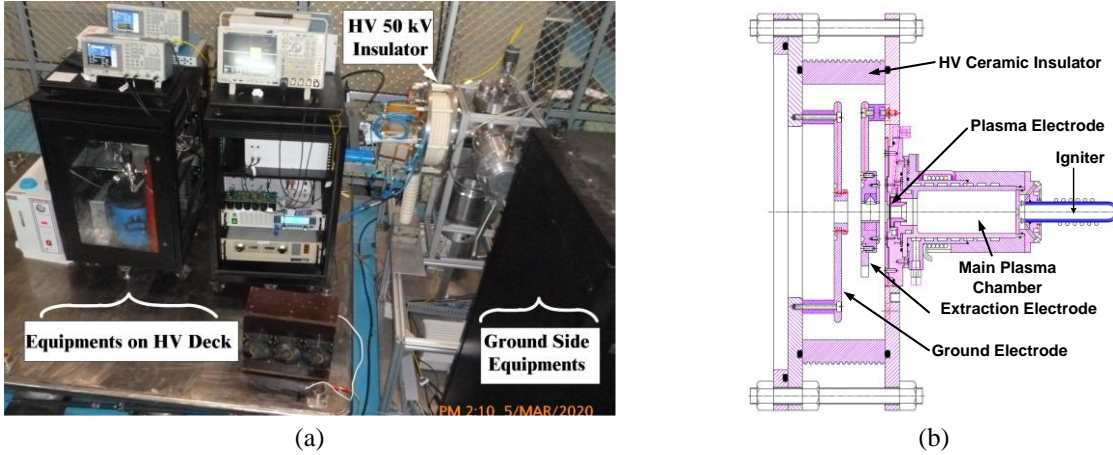


**FIGURE 1.** (a) The photograph of the experimental test setup of high duty factor RF based  $H^-$  ion source, and (b) The 2D-CAD drawing of RF based  $H^-$  ion source assembly.

### Hydrogen Ion Source Main Assembly

The photograph of the experimental test setup of high duty factor RF based  $H^-$  ion source is shown in Fig 1(a). It consists of three main sub-systems i.e. hydrogen plasma generating equipment's mounted on the high voltage deck, ion source assembly and other equipment's on the ground side. The  $H^-$  ion source tested for generating 11 mA ion beam current at 50 kV DC. The pulse width is 2 ms and the repetition rate is 50 Hz. The operating duty cycle is 10%. The pulsed igniter operated at 13.56 MHz and main plasma generator is operated at 2 MHz RF frequency. The 2D-CAD drawing of RF based  $H^-$  ion source assembly is shown in Fig. 1(b). The igniter tube has 10 turns forced air cooled RF antenna and main plasma chamber has 6 turns water cooled RF antenna and both are physically separated. The triode electrode geometry has been used for  $H^-$  ion beam extraction.

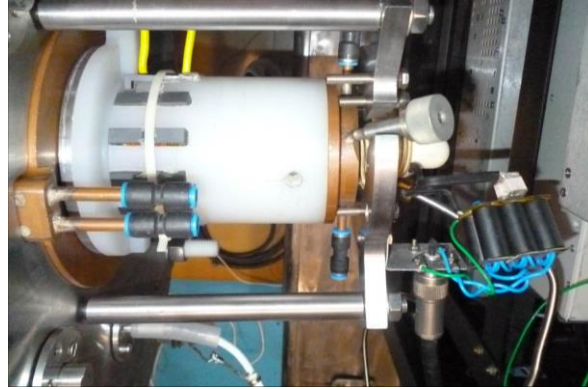
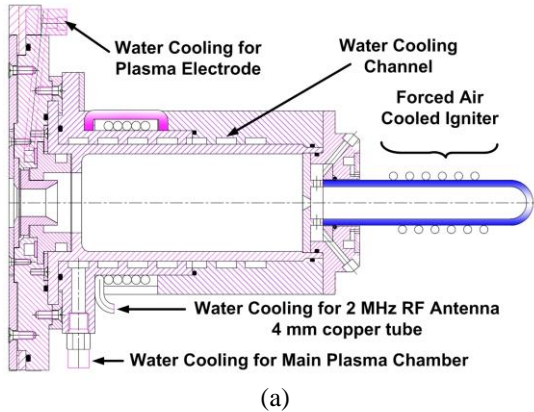


**FIGURE 2.** (a) 2D-CAD drawing of plasma electrode, plasma chamber and igniter tube, (b) The photograph of plasma generating chamber assembly.

### Cooling of Igniter, Plasma Chamber and Plasma Electrode

The main heat generating components are Igniter, plasma chamber, 2 MHz RF antenna and plasma electrode. The main plasma chamber is made of Aluminium Nitride, which is a high thermal conducting ceramic material and water cooled by outer spiral water jacket made of PEEK. The 2 MHz external RF antenna is made of 4 mm diameter copper tube insulated with kapton tape and PTFE tube and water cooling is provided with high voltage isolation. The plasma electrode is also water cooled. The 2D-CAD drawing of plasma electrode, plasma chamber and igniter tube are shown in Fig. 2(a). The photograph of plasma generating chamber assembly is shown in Fig. 2(b).

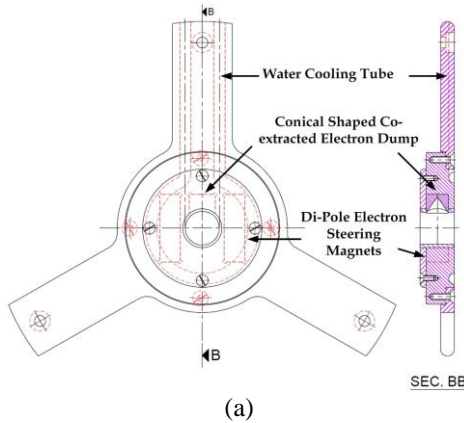


**FIGURE 3.** (a) The 2D-CAD drawings of extraction electrode, and (b) The photograph of extraction electrode with water cooling arrangement.

### Extraction Electrode Water Cooling

The 2D-CAD drawing of extraction electrode is shown in Fig. 3(a). Dipole filter field of 300 Gauss peak produced by permanent magnets is used for steering of co-extracted electrons. The electrons are terminated on a conical shaped molybdenum dump. The dumped electrons generate significant amount of heat and efficient cooling is required. The 6 mm copper tube was brazed for water cooling of extraction electrode and high voltage isolation was provided using high voltage feed through. The photograph of the extraction electrode with cooling arrangement is shown in Fig. 3(b). The extraction electrode tested for its insulation up to 15 kV DC.

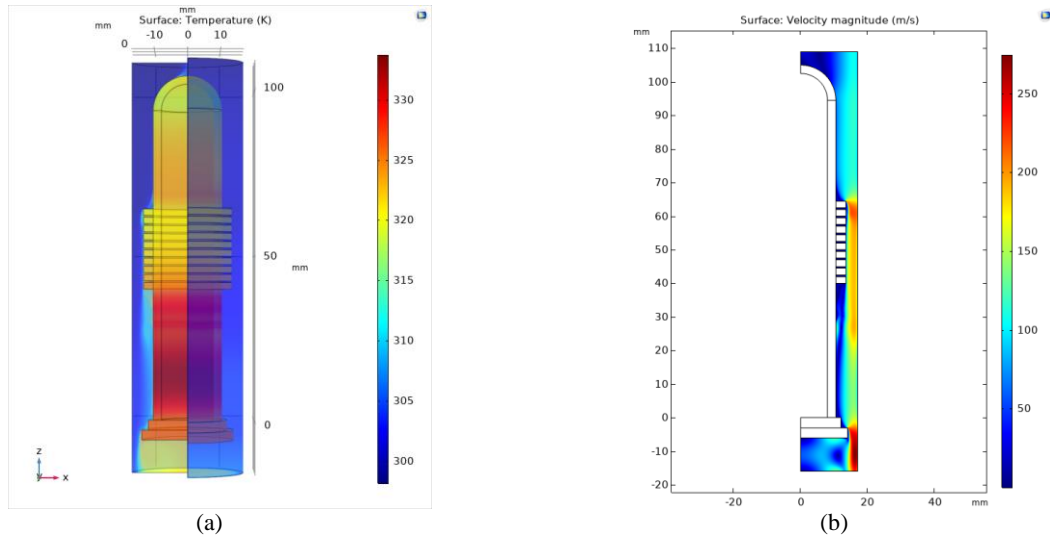


**FIGURE 4.** (a) Steady state thermal simulation showing 3D temperature distribution of igniter, (power loss on the inside tube is 60 W, air flow rate 80 CFM at 25 °C), (b) 2D-plot of air flow velocity (m/s) distribution around the igniter tube. X and Y axis 10 mm/div.

### Thermal Simulation of Igniter

The temperature rise in igniter tube was simulated using thermal module of COMSOL<sup>13</sup>. For simulation the average power loss is kept at 60 W, (13.56 MHz, 600 W RF power source was operated at 10% duty cycle) and the forced air cooling is provided with 80 Cubic Feet per Minute (CFM) instrument cooling fan with ambient temperature of 25 °C. The igniter tube outer diameter 22 mm, inner diameter 16 mm and length is 125 mm. The steady state thermal simulation showing 3D temperature distribution of igniter is shown in Fig. 4(a). The maximum temperature rise is ~ 60 °C, occurs in between the RF antenna and open end of tube. The 2D-plot of air flow velocity distribution around the ignitor tube is shown in Fig. 4(b).

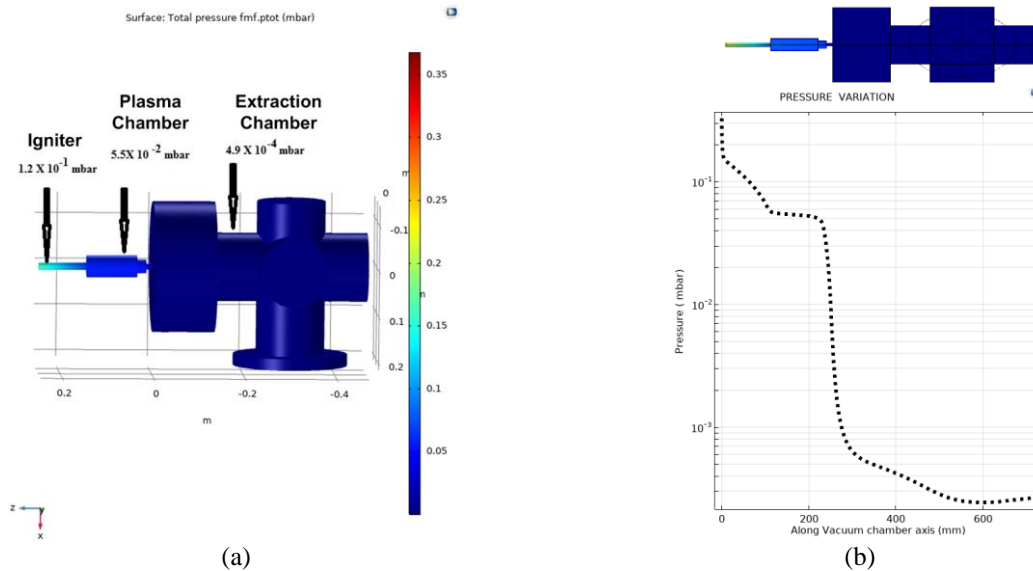


**FIGURE 5.** (a) Simulated 3D-plot of pressure for H<sup>-</sup> ion source. (b) Simulated pressure plot along the vacuum chamber axis of H<sup>-</sup> ion source. X-axis 200 mm/div. and Y-axis mbar/div.

## Vacuum Simulation with Hydrogen Gas

In order to get the required pressure in the igniter for pulsed ignition and main plasma chamber for required negative ion current generation, vacuum simulations were carried out using COMSOL Multi-physics vacuum module. The hydrogen gas purging rate is at 35 SCCM, in order to create high vacuum at extraction side and 0.1 mbar pressure in pulsed igniter tube, the igniter aperture diameter optimized to 3 mm with tube length 125 mm and the plasma electrode aperture diameter optimized to 6.5 mm with plasma tube length 135 mm. The vacuum is created using 3 numbers turbo molecular pumps ( $2 \times 500$  liter/sec. + 1700 litre/sec.). The simulation shows,  $1.2 \times 10^{-01}$  mbar hydrogen gas pressure in igniter tube which is sufficient for pulsed ignitor. The hydrogen gas pressure level in plasma chamber is  $5.5 \times 10^{-02}$  mbar, sufficient for enough plasma density for negative hydrogen current extraction and the extraction side vacuum is  $\sim 4.9 \times 10^{-04}$  mbar. The simulated 3D-plot of surface pressure in different part of  $H^-$  ion source is shown in Fig.5(a). The simulated pressure variation plot along the vacuum chamber (extraction) axis of  $H^-$  ion source is shown in Fig. 5(b). Large gradient in pressure recorded at the aperture of igniter and plasma electrode and minor gradient within igniter tube, plasma chamber and extraction chamber. There is three order of difference in vacuum level in between the igniter and extraction vacuum chamber. The extraction side vacuum level should be better for reducing the inter electrode unwanted arcing.

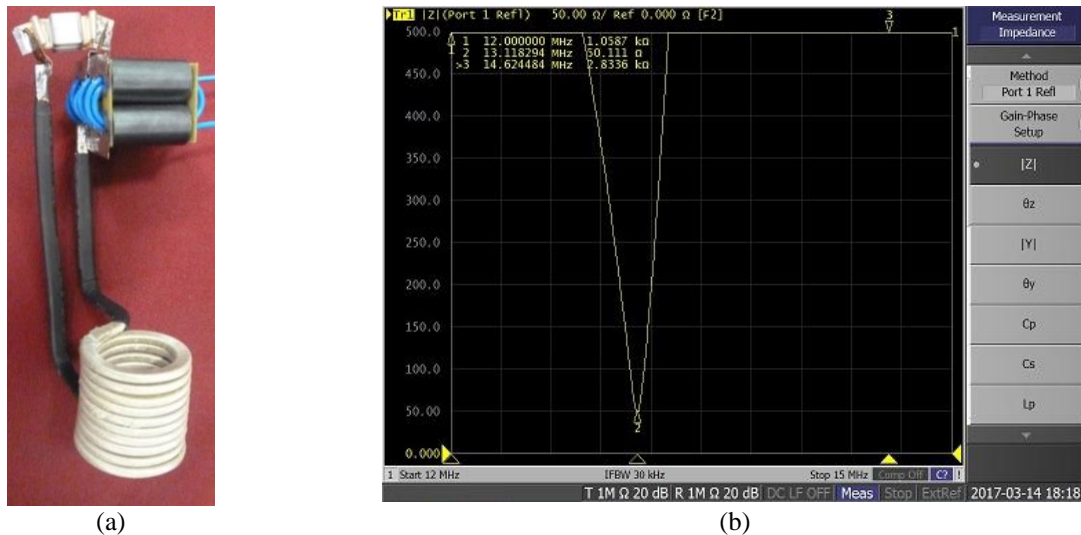


**FIGURE 6.** (a) A step-down RF transformer (turns ratio 9:1) and series resonance capacitor based 13.56 MHz RF matching network, and (b) The impedance of matching network measured with vector network analyser (VNA) is  $\sim 50 \Omega$ .

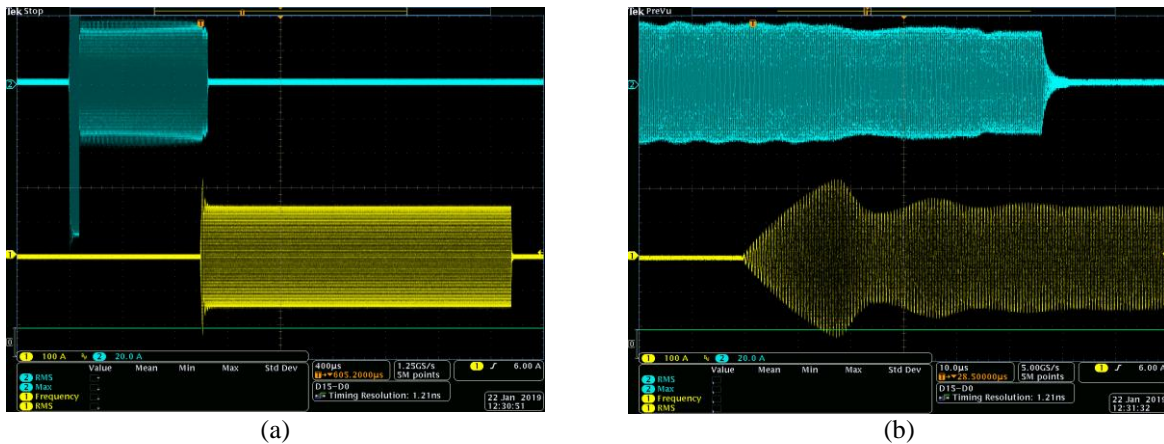


**FIGURE 7.** (a) The pulse width of 13.56 MHz RF power is 2 ms (minimum) Ch1 (green), and (b) Overlapping of 13.56 MHz Ch2 (green) and 2 MHz RF pulses Ch1 (yellow) for minimum 60  $\mu s$  time duration.

## Pulsed 13.56 MHz RF Igniter

The 13.56 MHz igniter was developed initially in continuous operation mode, as the igniter is used only fraction of time for initiation of main plasma discharge, hence major efforts were put to develop a pulsed mode igniter. For this, the major changes were incorporated to operate the igniter in pulsed mode, are (i) the transformer based matching network was developed, photograph is as shown in Fig. 6(a), (ii) the impedance of RF antenna without plasma adjusted near to  $50 \Omega$ . The recorded impedance plot of matching network is shown in Fig. 6(b), (iii) the maximum magnetic motive force generated is  $\sim 800$  Amp-Turns, (iv) the pulsed RF 13.56 MHz power is kept “ON” for minimum 2 ms duration as shown in Fig. 7(a), (v) over lapping of two RF pulses (13.56 MHz and 2 MHz) for minimum  $60 \mu\text{s}$  duration as shown in Fig. 7(b), and (vi) The 13.56 MHz RF antenna closely wound on the alumina igniter tube.

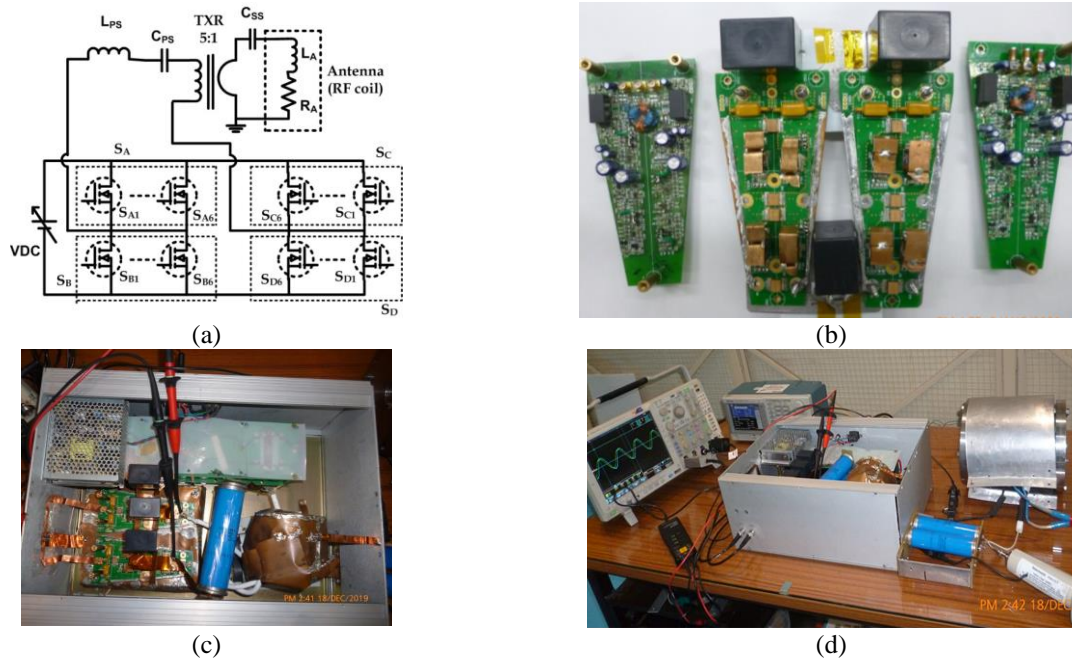


**FIGURE 8.** (a) 2 MHz pulsed RF source circuit diagram, (b) Photograph of full-bridge SiC-MOSFETs using two half-bridges and its isolated gate driver circuit boards, (c) 2 MHz pulsed RF source assembled in 4 U, 19” electronics casing, and (d) Photograph of the 2 MHz pulsed RF source test setup with dummy load.

## Solid State 2 MHz Pulsed RF Source

The 2 MHz pulsed RF source was developed using 24 numbers of SiC-MOSFETs. The MOSFETs are connected in full-bridge configuration. The 2 MHz pulsed RF source circuit diagram is shown in Fig. 8(a), this converts DC voltage into 2 MHz rectangular voltage pulses with variable amplitude. Two series resonant components convert these rectangular voltage pulses into sinusoidal current pulses in RF antenna. The inverter current is amplified by step-down isolation RF transformer. The RF power is controlled by varying input DC voltage. The photograph of full-bridge SiC-MOSFETs using two half-bridges and its isolated gate driver circuit boards are shown Fig. 8(b). The SiC-MOSFETs were soldered to copper heat sink for removing heat with forced air cooling. The SiC-MOSFETs are switched at 2 MHz with nearly 50% duty cycle within 2 ms Pulse duration, as SiC-MOSFETs are switched in “ON” or “OFF” mode, hence losses are minimum. 2 MHz pulsed RF source is assembled in 4U, 19” standard electronic casing is shown in Fig. 8(c). It consists of DC bulk capacitor bank for energy storage, SiC-MOSFETs in full-bridge inverter configuration for switching, primary and secondary series resonant components and step-down isolation RF transformer to step-up the current. The 2 MHz pulsed RF source was tested with dummy load at full 100 kW RF power level. The photograph of the 2 MHz pulsed RF source test setup with dummy load is shown in Fig. 8(d). The RF antenna is provided with water cooling arrangement and switching SiC-MOSFETs, resonant components and RF transformer are forced air cooled.

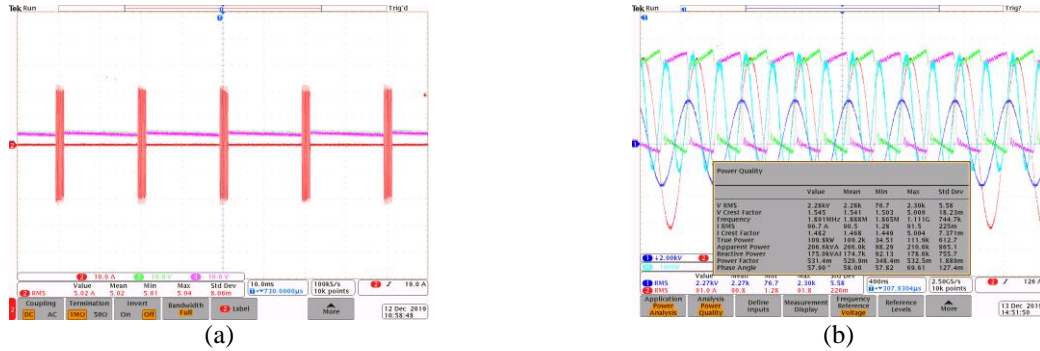


**FIGURE 9.** (a) Recorded waveform of 2 ms pulse width at 50 Hz repetition rate with peak RF power of 100 kW, and (b) RF power measurement using antenna voltage and current. 2 MHz RF antenna voltage (Ch-1 blue 2 kV/div.), Current (Ch-2 red 50 A/div.) and Inverter output voltage (Ch-3 green and Ch-4 pink color) 50 V/div.

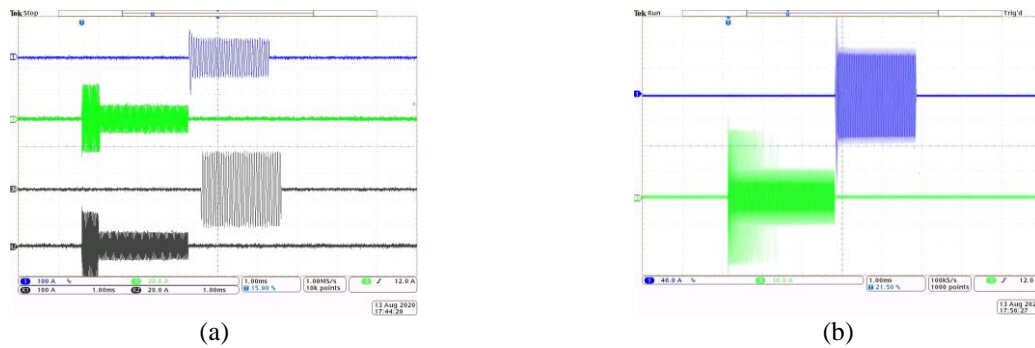


**FIGURE 10.** (a) Recorded waveform Ch1 (light blue): 2 MHz antenna current, 100 A/div. Ch2 (green): 13.56 MHz antenna current, 20 A/div. Main plasma starts reliably. ChR1 (grey): 2 MHz antenna current, 100 A/div. ChR2 (black): 13.56 MHz antenna current, 20 A/div. Main plasma failed to start, and (b) Recorded persistence mode view for 2 MHz antenna current (blue) and 13.56 MHz antenna current (green).

2 MHz pulsed RF source tested with dummy load at full RF power at 10% duty factor with 50 Hz repetition rate. The recorded waveform is shown in Fig. 9(a). The RF antenna current (Ch1) and voltage (Ch2) along with SiC-MOSFETs full bridge output voltage (Ch3 and Ch4) recorded waveforms are shown in Fig. 9(b). It delivers 90 A RMS current through 2 MHz RF antenna and delivers 100 kW RF power to the dummy load. Figure 10(a) shows the RF pulse timing of 13.56 MHz pulsed igniter and 2 MHz main plasma generator, if there is proper over lapping of these two pulses the main plasma starts reliably (Ch1 and Ch2), if there is delay in between these two pulses main plasma fails to start (ChR1 and ChR2). In order to check the igniter inception behaviour, antenna current recorded in persistence mode shown in Fig.10(b). The igniter starts within 1.2 ms reliably without failure during 2 ms RF pulse.

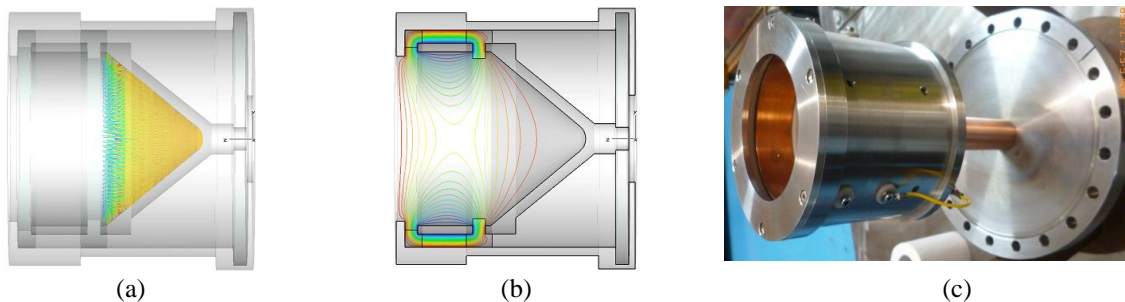


**FIGURE 11.** (a) The trajectories of the secondary electron emission from the collector surface of the Faraday cup, when ring is biased at 100 V (b) The distribution of the isoline of the potential in the Faraday cup, when ring is biased at 100 V, and (c) The photograph of the water cooled Faraday cup.

A cone type Faraday cup was designed and developed using Microwave Studio CST-EM<sup>14</sup> software with particle tracking solver module. A biasing ring is used to prevent the secondary electrons escape from the surface of the collector and cone shape collector, where incident beam terminates. The Faraday cup opening diameter is 76 mm, cone length is 50 mm and made of OFE copper. The trajectories of the secondary electron emission from the collector surface of the Faraday cup, when ring is biased at 100 V is shown in Fig. 11(a). The distribution of the isoline of the potential in the Faraday cup, when ring is biased at 100 V is shown in Fig. 11(b). The photograph of the water cooled Faraday cup is shown in Fig. 11(c).

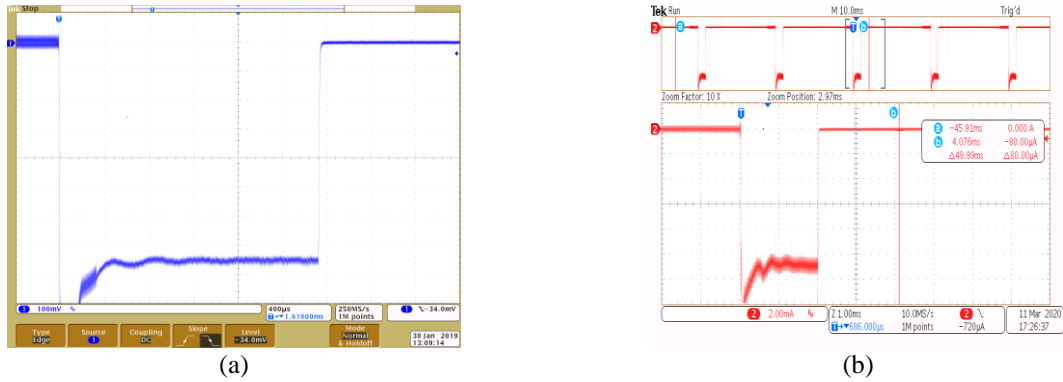


**FIGURE 12.** (a) The recorded waveform of pulsed  $H^+$  ion beam current  $\sim 15$  mA, with 2 ms pulse width at 2 Hz repetition rate, ( 0.4% duty factor) at 50 kV DC accelerating voltage, Scale :X-axis : 0.4 ms/div. and Y-axis : 4.0 mA/div., and (b) recorded waveform of pulsed  $H^+$  ion beam current  $\sim 11$  mA with 2 ms pulse width at 50 Hz repetition rate, (10% duty factor) at 50 kV DC accelerating voltage, Scale :X-axis : 1.0 ms/div. and Y-axis : 2.0 mA/div.

The recorded waveform of pulsed  $H^+$  ion beam current was 15 mA at 2 Hz repetition rate with 0.4% duty factor and 11 mA at 50 Hz with 10% duty factor at 50 keV beam energy as shown in Fig. 12(a) and (b), respectively.

## CONCLUSION

The pulsed RF source at 2 MHz, 100 kW was successfully demonstrated at 2 ms pulse width, 50 Hz repetition rate (10% duty factor). The RF source major components like RF antenna and matching network were designed and developed successfully. The measured  $H^+$  ion current was 15 mA at 2 Hz repetition rate, 0.4% duty factor and 11 mA at 50 Hz, 10% duty factor at 50 keV beam energy. The beam current was dumped in a water-cooled Faraday cup. To operate ion source with high duty factor main heat generating components like main plasma chamber, 2 MHz RF antenna, plasma electrode and extraction electrode were water cooled and igniter, 13.56 RF antenna and matching networks, 2 MHz RF source and its matching network, current stabilizing network of high voltage power supplies were forced air cooled.

## ACKNOWLEDGMENTS

The authors would like to appreciate the help received from Shri Bharat Kumar Arya, Shri Ranjan Kumar, Shri Rajesh Nagdeve, Shri Sanjay Singh, Shri Murtiram Meena, Shri Om Prakash and Shri S. K. Sonawane during various stages of development of the external antenna RF based pulsed  $H^+$  ion source.

## REFERENCES

1. M.P. Stockli, R.F. Welton, and B. Han, Rev. Sci. Instrum. 89, 052202 (2018).
2. R. F. Welton, V. G. Dudnikov, K. R. Gawne, B. X. Han, S. N. Murray, T. R. Pennisi, R. T. Roseberry, M. Santana, M. P. Stockli, and M. W. Turvey, Rev. Sci. Instrum. 83, 02A725 (2012).
3. J. Peters, Rev. Sci. Instrum. 79, 02A515 (2008).
4. T. Schenkel, J. W. Staples, R. W. Thomae, J. Reijonen, R. A. Gough, K. N. Leung, R. Keller, R. Welton, and M. Stockli, Rev. Sci. Instrum. 73, 1017 (2002).
5. Rajnish Kumar, Dharmraj. V. Ghodke, and V. K. Senecha Rev. Sci. Instrum. 88, 083302 (2017).



6. Dharmraj. V. Ghodke, R. K. Khare, Rajnish Kumar, Manish Pathak, S. K. Jain, Ajith Amban, K. Murali Krishnan, and V. K. Senecha *Rev. Sci. Instrum.* **91**, 043506 (2020).
7. J. Lettry, D. Aguglia, J. Alessi, P. Andersson, S. Bertolo, S. Briefi, A. Butterworth, Y. Coutron, et al, *Rev. Sci. Instrum.* **87**, 02B139 (2016).
8. M. P. Stockli, B. Han, S. N. Murray, T. R. Pennisi, C. Piller, M. Santana, and R. Welton, *Rev. Sci. Instrum.* **87**, 02B140 (2016).
9. J. Lettry, S. Bertolo, U. Fantz, R. Guida, K. Kapus et al et al, *AIP Conference Proceedings* 2052, 050008 (2018).
10. Manish Pathak, V. K. Senecha, Rajnish Kumar, Dharmraj. V. Ghodke, NIMA838, 96 (2016).
11. Nayan Kumar Gunele, Sandeep Bhongade, D. V. Ghodke, R. M. Vadjikar, V. K. Senecha and S. C. Joshi, 4<sup>th</sup> IEEE Applied Electromagnetic Conf., KIIT University, Bhubaneswar (2013).
12. S. Briefi, S. Mattei, J. Lettry, and U. Fantz, *AIP Conference Proceedings* 1869, 030016 (2017).
13. <https://www.comsol.co.in>
14. <http://www.cst.com/products/cstmws>